Thermo-Mechanical Modeling of Single High Power Diode Laser Welds

E. A. Bonifaz, PhD
Departamento de Ingeniería Mecánica de la Universidad San Francisco de Quito, Casilla Postal: 17-12-841 Círculo de Cumbayá, Quito, Ecuador, edisonb@usfq.edu.ec

J. E. Indacochea, PhD
University of Illinois at Chicago, Dept. of Civil and Materials Engineering (MC 246) College of Engineering, 842 West Taylor Street, Chicago-Illinois 60607-7023, jeindaco@uic.edu

Abstract
High Power Diode Laser (HPDL) systems could become viable alternatives to resistance welding prevalent in a variety of industries [1]. Recent progress in available beam power and beam quality has meant that high power diode lasers (HPDL) may soon become prime tools for welding in many assembly applications for industrial production. With this in mind, the aim of this study was to characterize the weld size, shape, and thermo-mechanical history as a function of the laser operating parameters, of single high power diode laser welds in low-carbon steel sheets by mathematical modeling. A three-dimensional finite element model has been developed to simulate the diode laser welding process and predicts the final distortions of a single pass weld. The finite element calculations were performed using ABAQUS® FE code, which takes into account thermal and mechanical behavior. Unlike other three-dimensional analysis, the current work takes into account a moving heat source in the beam rectangular profile with a "top-hat" intensity distribution in one beam direction ("slow-axis") and a Gaussian curvature in the other ("fast-axis"). The mathematical modeling has been investigated with a view to generate numerical data to define an optimum parameter space for an on-going experimental project of such welds. The size, shape, hardness, strength and microstructure of the welds analyzed as a function of laser parameters such as laser power, welding time and welding speed, is currently underway and will be published later.

Keywords
Laser welds, ABAQUS®, Top-hat distribution

1. Introduction

Industry has already started to integrate diode laser technology into manufacturing because of the compact shape and the beam produced, which can be expanded to a larger rectangular beam [2]. One advantage over the CO_2 Laser is the short wavelength (808 nm and/or 940 nm), which leads to higher absorption. Compared with the NdYAG laser, the major advantages are to be found in the beam profile, and in the significantly lower investment and operating costs that result from the high efficiency [3]. Their compact size and low weight makes them particularly suitable for use in conjunction with robotic control. The advantages of laser welding over conventional welding techniques include more reproducible welds, smaller heat affected zones and lower distortion at high welding speeds. The technology has now advanced to such an extent that it is possible to produce laser beams of sufficiently high power density to induce the melting and welding of sheet metal.

Because of their unique features, e.g. small size and low weight which makes them easy to integrate, and because of their high efficiency and reliability which leads to low running costs, diode lasers gained high interest as a pump source for solid-sate-lasers as well as a new laser source for materials processing [4]. In diode lasers, the individual sectors may emit different power levels because of manufacturing tolerances in the semiconductor material and the complex structure. The special shape of the light generation area leads to special light emitting characteristics, which shows a high divergence in the direction of the pn-transition ("fast axis") and a lower divergence, but a wide emitting "stripe" in the other ("slow axis"), as represented in Figure 1.

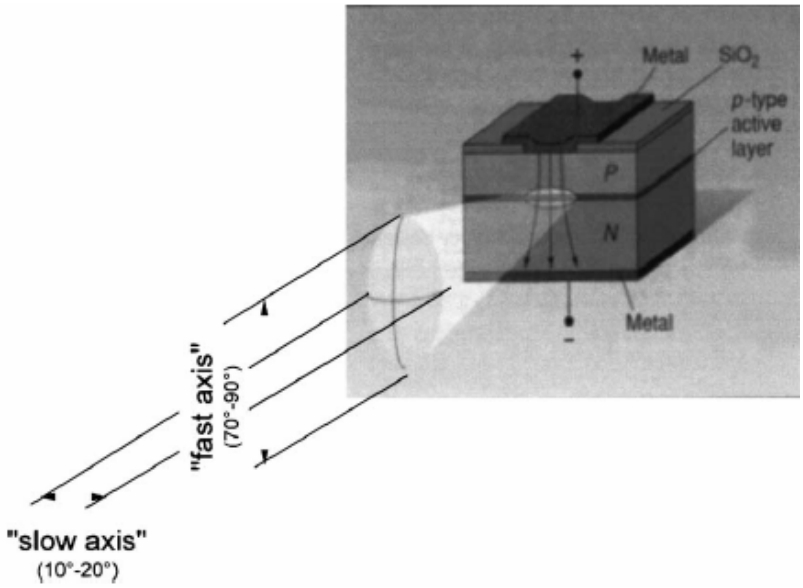

Figure 1: Scheme of light generation in a pn-transition of a laser diode [4].

From the far field distributions it is also visible the beam quality in the fast axis is almost diffraction limited and shows a Gaussian intensity distribution, on the other hand the intensity distribution in the slow axis reflects the irregularity in the emission and also the rather poor beam quality (Figure 2). This fact is one of the key limitations for the brilliance of high power diode lasers [4].

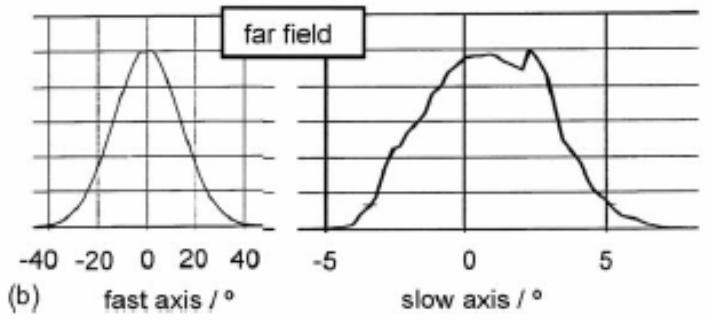

Figure 2: Beam emission characteristics of a diode laser bar: fast axis is almost diffraction limited with a Gaussian intensity distribution [4].

The beam profile of a high power diode laser shows typically a rectangular shape with a "top-hat" intensity distribution in one beam direction ("slow-axis") and a Gaussian curvature in the other ("fast-axis") as shown in Figure 3. Because of its rectangular shape, the HPDL beam is especially well suited for

surface hardening application. However, it is also well suited for high speed deep penetration welding as demonstrated recently by Petring [5].

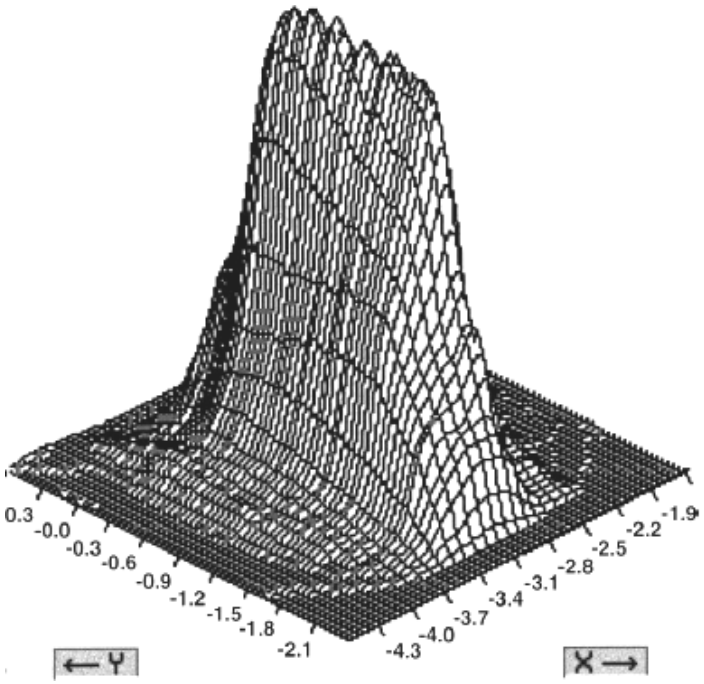

Figure 3: Typical energy distribution in the focal plane of a high power diode laser [4].

2. The Welding Process

Welding technology is the main joining technique used in industry for parts assembly in cars, ships, planes, trains or civil engineering machines. Numerous welding problems, particularly those concerning safety in the nuclear industry, are related to residual stresses. One major industrial concern is to limit the use of clamping tools. The result is a direct cost reduction but it also eases the automation of assembly lines. Optimization of the welding sequence and process is a way to reach this goal. However, the experimental optimization of the welding technique regarding distortions requires prototyping and measurements which are extremely expensive and time consuming and in which ultimately, very few solutions are possible. Moreover, additional machining after welding or pre-distortion is often still required. Finite element simulations can be used to optimize the weld heat input and minimize the distortions, but this task is quite difficult in view. On one hand, that welding processes involve complex couplings between heat transfer and the metallurgical changes experienced by the base metal. On the other hand, that where local models are sufficient to predict stresses, only global 3D models can correctly predict distortions. Considering the high gradients of temperature, microstructure, stresses and plastic strains located in small areas that are involved in welding simulations, the refinement of meshes near the welding line increases drastically the models size and consequently leads to unreasonable computation times [6].

The most critical input data required for welding thermal analysis are the parameters that describe the heat input to the weldment from the heat source. Distortion, residual stresses, grain structure, cooling rates, high temperatures and consequently the reduced strength of a structure in and around a weld joint is produced by the localized thermal cycle caused by the intense heat input of fusion welding. Reducing the heat input to the work piece is a primary goal for weld process selection and weld schedule development for all welding applications particularly in the aerospace and electronics industry. For example in micro

welding applications, the depth of penetration is typically less than 1.0 mm, and hermeticity rather than mechanical strength is the primary joining requirement [7], hence the control and selection of the weld heat input is most critical.

With the virtual prediction of distortions and residual stresses of a welded part, the process can be optimized in the early stage of prototyping. By leading comparison between the simulation performed by a finite element code and the real process, the simulations can be conducted by carrying out simultaneous iterative modification of the welding sequence in order to improve the manufacturing process for distortion and residual stresses. Transient thermal histories and HAZ size can be compared with experimental work to be feedback into the interacting model/weld fabrication system so as to optimize the welding process. The optimization process requires running one computation for each evaluated modification. For this reason simulations are expected to last at most few hours and not days or weeks. On the other hand, Vickers micro-hardness indenters serve as a baseline for comparison. Residual stresses and metallurgical states obtained from simulations should be compared vis-à-vis with standard experimental work to get the optimal solution. In time, this help in the decision making process to establish the optimum design parameters combination.

2.1 Computational Model

The primary objective of a thermo-mechanical welding model is to predict the deformations of an actual welded part. To achieve this goal, materials elastic-plastic properties, temperature dependent materials properties, volume changes due to phase changes, heat losses to the surrounding, etc., must be included in the model.

In a first stage, a methodology is developed to perform complex 3D non linear transient finite element welding simulations, using modeling considerations described in the next section. The methodology allows calculating residual distortions to enable optimization of the welding sequence reducing prototyping. The method rests upon a coarse global 3D (7500 eight nodded brick elements - DC3D8 and C3D8 ABAQUS® elements) approach for the modeling of the physical phenomena induced by welding. Typically, transient problems are numerically solved using time-increment approach with the number of increments varying from hundreds to thousands, depending on the nature of the problem (Lagrangian formulation). The transient analysis stops when steady state is achieved. Since at the present date, computer-processing speed is not cost prohibitive, a transient Lagrangian formulation (which is more realistic than steady state Eulerian formulations), was used in the finite element modeling.

2.1.1 Modeling Considerations

1) Two important parameters in all models of welding are the fraction of incident energy from the laser beam that is actually absorbed by the material and the amount subsequently used to melt the metal. The energy transfer efficiency η is defined as the ratio of the heat absorbed by the workpiece and the laser output power.

$$\eta = \frac{heat\ \ absorbed\ by\ the\ workpiece}{laser\ output\ \ power} x100\% \tag{1}$$

The melting efficiency η_m is defined as the ratio of the energy used for melting the metal and the heat input. For seam welds the melting efficiency is given by Fuerschbach [8] as

$$\eta_m = \frac{vA\delta h}{\eta q_0} \tag{2}$$

Where v is the welding speed, q_o is the laser output power, A is the cross-sectional area of the weld fusion zone and δh is the enthalpy of melting. Although the transfer efficiency is not known, the product $\eta\eta_m$ could be calculated from the fusion zone volume or area for each weld. These values are given in ref. [1], for the various laser operating powers. A value of 10.4 J/mm^3 given for 1018 low-carbon steel was used in ref. [1] for δh. The values of energy transfer efficiencies dependent on the laser power and shielding gas documented in Table 1 were estimated by Walsh et.al. [1] by fitting the equation of a material-independent model for the efficiency in terms of two dimensionless parameters to the data for stitch welds.

Table 1. Energy transfer efficiencies (η) for the diode laser stitch welds [1].

Laser Power (KW)	Efficiency – with shielding gas	Efficiency – without shielding gas
1.4	0.64	0.38
2.26	0.57	0.43
1.4 and 2.26	0.57	0.42

2) A literature review reveals that the term melting efficiency had never been related to the welding process variables in a FEM simulation [7]. Also, it appears that, up to the present time, the quantitative treatment for representing heat flow in weld deposits and pool convection (fluid motion) in a 3D (nonlinear-transient) space has been limited. The reason for this is the difficulty in developing a meaningful relationship between theoretical models and experimental observations. To enhance the research, the decoupled heat equation of Navier-Stokes or magnetohydrodynamic (MHD) equations is used with heat flux per unit area per unit time $q(x,z,t)$ and effective thermal conductivity K_{eff} . More precisely, the traditional Gaussian moving heat source model (Eq.3) and K_{eff} functions reported elsewhere, are tested using a developed ABAQUS® user's subroutine. In the present work, thermal efficiency was used to quantify the energy made available by the heat source through the energy input rate Q, i.e., $Q = \eta\eta_m q_o$. When high wall plug efficiency is introduced in the decoupled heat equation, the electrical to optical conversion that varies from 30% to 60% is incorporated in the heat transfer analysis.

$$q(x,z,t) = \frac{3Q}{\pi c^2} \exp\{-3[(z-vt)^2 + x^2]/c^2\} \tag{3}$$

Here, c = the characteristic radius of flux distribution (mm); v = the beam laser speed (mm/s), t = time (s).

3) Boundary conditions are employed to account for surface heat losses (natural convective heat transfer, quantum Stefan-Boltzman radiation and forced convection due to the flow of the shielding gas).

4) All thermo physical properties are considered to be temperature dependent.

5) Large deformations and large strains are accounted for and an additive decomposition of the elastic, plastic and thermal strain rates

$$\dot{\varepsilon}^{tot} = \dot{\varepsilon}^{e} + \dot{\varepsilon}^{p} + \dot{\varepsilon}^{th} \tag{4}$$

6) The FEM code ABAQUS® was used in all simulations. ABAQUS® computes dimensional variations and distortions of parts, strength and deformability of the material in use and residual stresses, during and at the end of the welding process.

2.1.2. Modeling Setup

A 2500 watts direct diode laser power, found to work well for most carbon steels welds, was used in this modeling. The geometry of the workpiece is 100 x 60 x 5 mm. The welding speed was kept constant and assumed to have a magnitude of 30 mm/s [6]. The plate was fixed as a cantilever beam to observe the

bending behavior during and after the welding process. The schematic of the weld set up for modeling and details of the elements are shown in Figure 4.

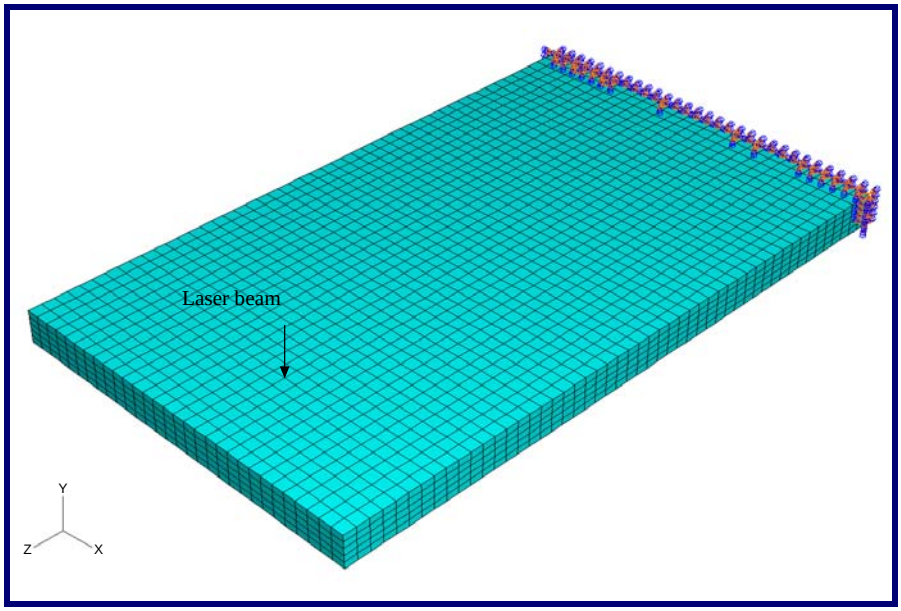

Figure 4: 60 x 5 x 100 mm finite element mesh consisting of 7500 eight-nodded elements. Each element of the mesh has a volume of 2 x1 x 2 mm.

2.1.3 The heat flux model

The diode laser heat flux distribution was calculated with Eq. (3) and applied to eight rows (two elements each) for a total period of time equal to 0.6 s. Each row was exposed to the laser beam during a time of 0.133 s (i.e., t = 2*c*/*v*, *c* = 2 mm and *v* = 30 mm/s). The heat flux loading profile in the fast and slow axis is shown in Figure 5.

2.2 Material Model

Commercial 1010 carbon steels have been selected as test materials. The thermo physical properties used in the finite element model are according to Frewin and Scott [9]. The plastic behavior of the material is described by the Von Mises yield function and hardening was accounted for. A Young's Modulus E = 207E3 MPa, a thermal expansion coefficient equal to 14E-6/^{o}C and the yield stress σ_y equal to 250 MPa (for temperatures equal to 121 ^{o}C) and σ_y = 27 MPa (for temperatures equal to 1111 ^{o}C) were used in the analysis.

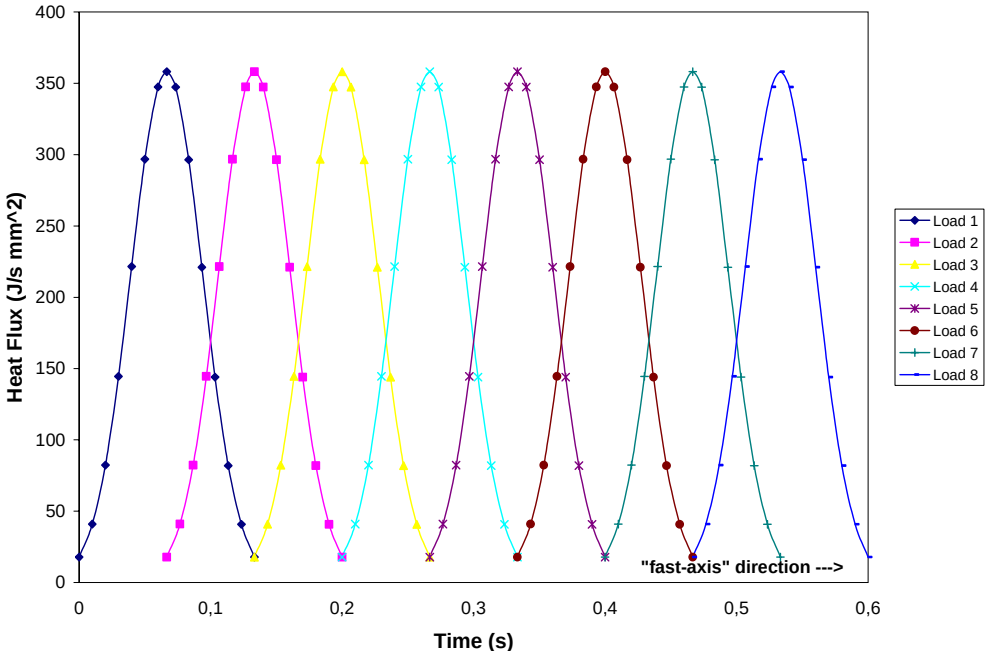

(a)

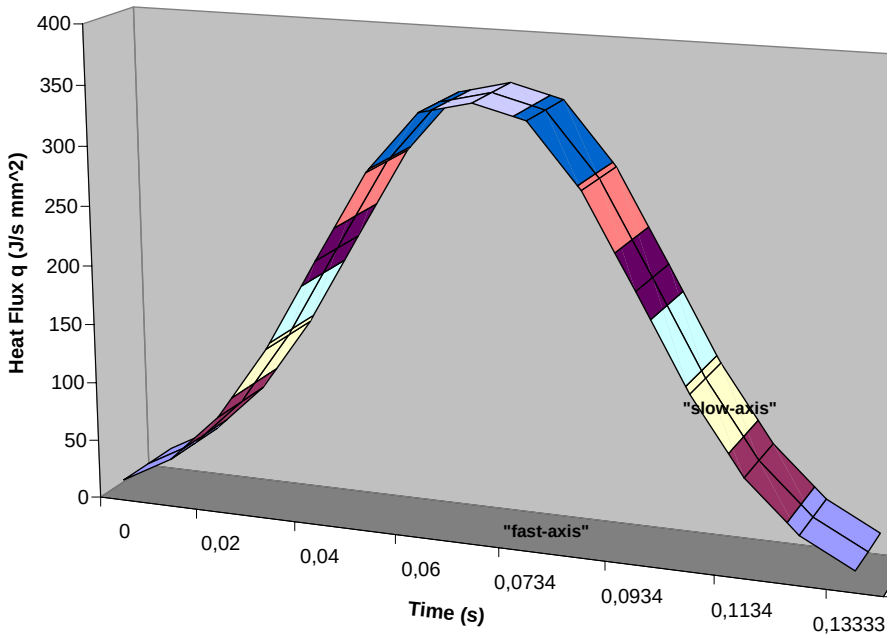

(b)

Figure 5. a) Intensity loading profile of high power diode laser beam - "fast-axis" direction. b) Heat flux loading profile both in the "fast-axis" and in the "slow axis.

3. Results and Discussion

The model was run for both the duration of the applied heat flux and the subsequent cooling period. The computational time for the thermo-mechanical FEM-model was approximately 1 hour and was performed on a Pentium III PC with 256 MB ram. Figure 6 shows the thermal contours at three different *heating* sequences for a typical laser welding operation.

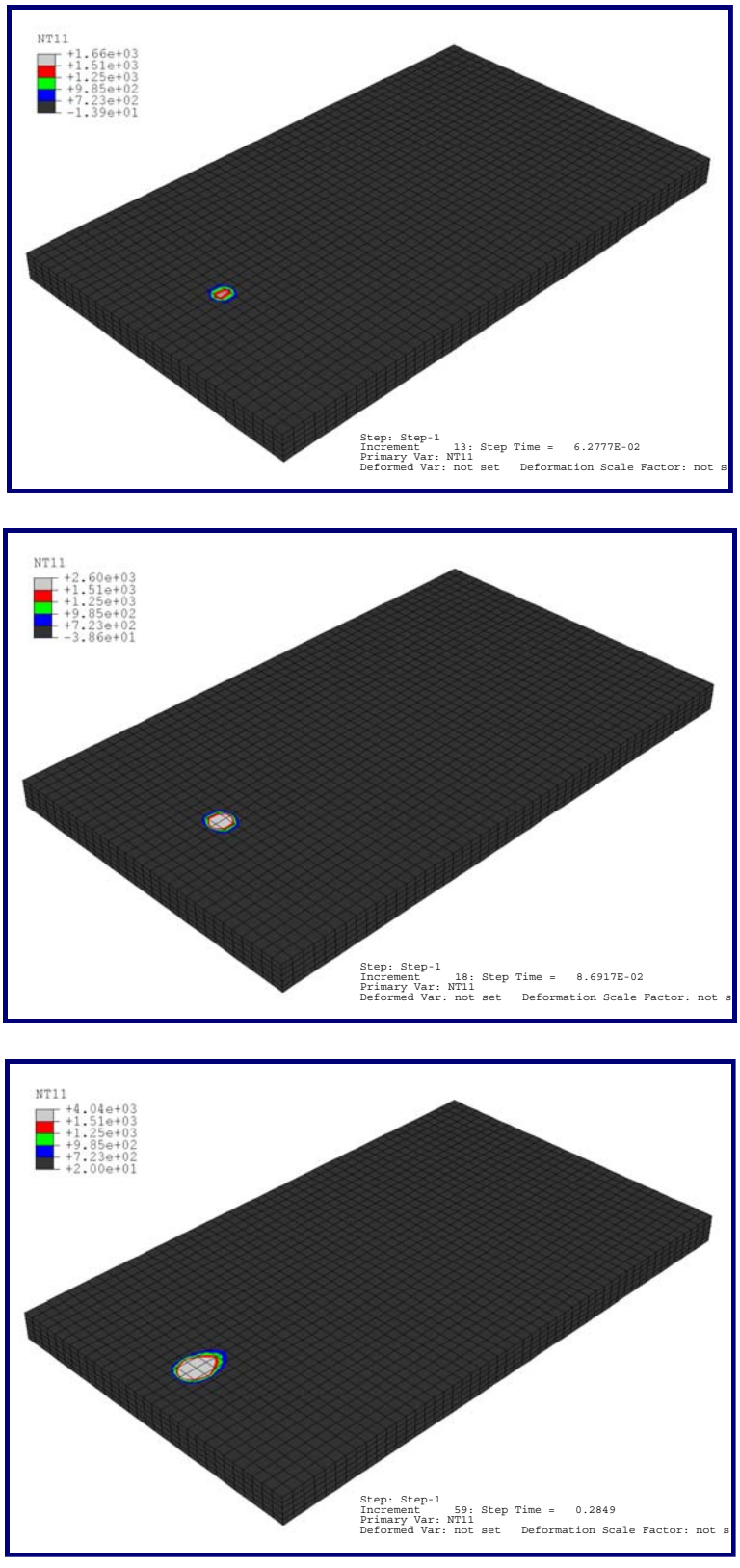

Figure 6. Temperature distribution during welding process at three different heating sequences. Step time (s) documented in figures.

Figure 7 shows the thermal contours at three different *cooling* sequences. Note the difference in contour values and weld shape when compared with the heating sequence in Figure 6.

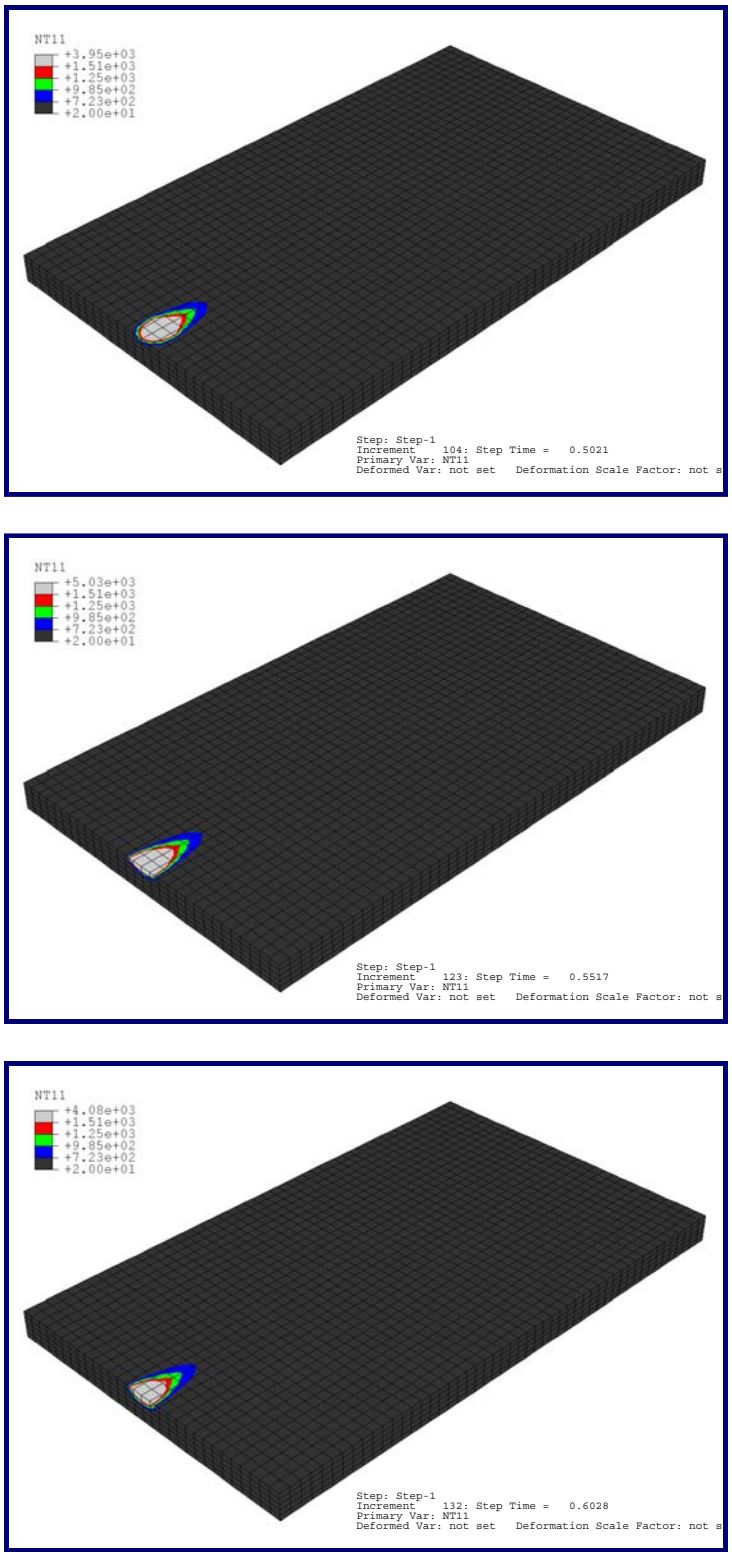

Figure 7. Temperature distribution during welding process at three different cooling sequences. Step time (s) documented in figures.

The influence of welding speed on isotherm shape is clearly observed. The shaded zone indicates the fusion and heat affected zone range. Figures 6 and 7 show a comparison between the isotherm distributions at different time steps for a high welding speed for carbon steel. As expected, the higher welding speed predicts a narrower weld deposit. On the other hand, the uniformity of the weld deposit is attributed to the special top hat Gaussian distribution of diode lasers.

Thermal history of the material is very important in determining the microstructural changes the material undergoes and the strength of the weld joint. Any suspected critical region can be analyzed by plotting the thermal history in that region. As a matter of fact, Tekriwal and Mazumder's results [10] indicate that the cooling of the metal adjacent to the weld pool is the critical metallurgical location. To enhance the research efforts, in this study, a new mathematical model has been developed with a view to generate numerical data to define an optimum parameter space for an on-going experimental project of such welds. Very high temperatures cannot be measured by simple techniques such as thermocouples. Yet, in the region away from the molten zone, the temperature can be measured and compared in order to get some idea of the accuracy of the numerical results. To contribute with the numerical approach, thermal contours and thermal histories of three sample points at time 0.9 s. are drawn in Figure 8. The heating/ cooling curves of the three central axis surfaces nodes at positions 0, 2 and 4 mm from the end of the specimen, indicate that the critical position corresponds with the node located at the end of the weld deposit.

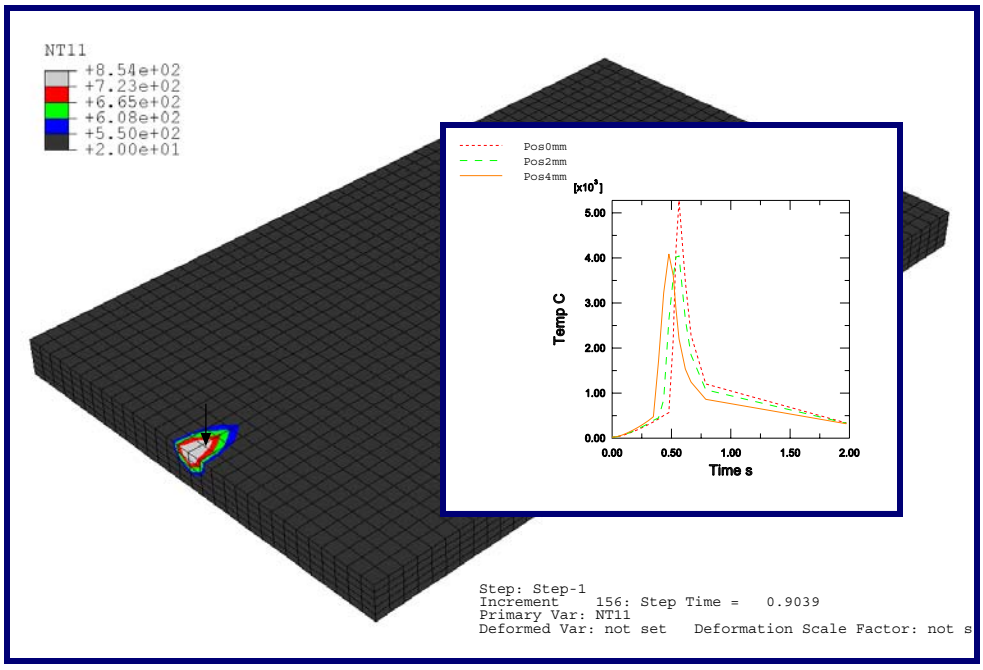

Figure 8. Thermal contours and thermal histories for three different positions at time 0.9 s.

This thermo-mechanical model was also used to develop the state of residual stresses following welding. Figure 9 shows contours of Misses stresses at time 40 s. It is interesting to note that in positions close to the crater formation (end of the specimen), high values of Misses stresses remain after the specimen reached the steady state, that is, after 40 s. It is clear to conclude that the heating/cooling critical position is the responsible for the creation of high values of residual stresses found at the end of the specimen.

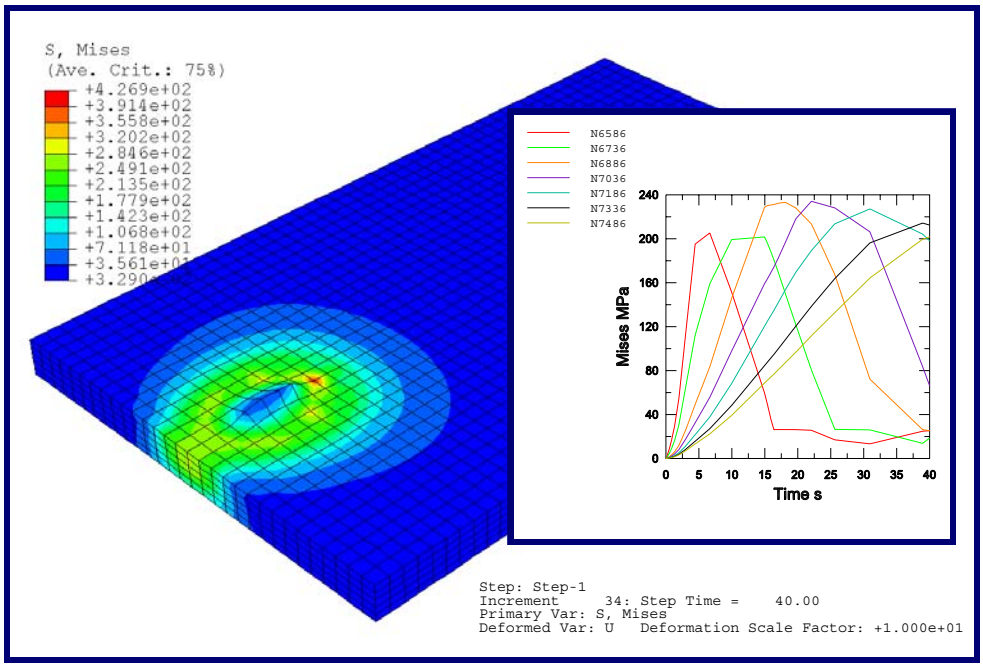

Fig. 9. Misses stresses contours and mechanical histories after the specimen reached the steady state.

4. Concluding Remarks

A three-dimensional finite element model has been developed to simulate the diode laser welding process and predicts the final distortions of a single pass weld. The finite element calculations were performed using ABAQUS® FE code, which takes into account thermal and mechanical behavior. Unlike other three-dimensional analysis, the current work takes into account a moving heat source in the beam rectangular profile with a "top-hat" intensity distribution in one beam direction ("slow-axis") and a Gaussian curvature in the other ("fast-axis") as shown in Figure 3. The size, shape, hardness, strength and microstructure of the welds analyzed as a function of laser parameters such as laser power, welding time and welding speed, is currently underway and will be published later.

5. Acknowledgements

E. A. Bonifaz is grateful with the University of Illinois at Chicago and with the Fulbright Visiting Scholar Program (GRANT NUMBER 68427790), for the financial support provided.

References

[1] C.A. Walsh, H.K.D.H. Bhadeshia, A. Lau, B. Matthias, R. Oesterlein, and J. Drechsel, *Cambridge University Publications.*

[2] http://www.industrial-lasers.com/archive/2000/06/0600fea3.html

[3] http://www.rofin.com/english/anwendungen/macro/haerten/index.htm

[4] F. Bachmann, *Applied Surface Science*, 208-209 (2003) 125-136.

[5] D. Petring, *LaserOpto*, 31 (5) (1999) 6.

[6] D. Berglund (2003). Private Communications

[7] E. A. Bonifaz, "Finite Element Analysis of Heat Flow in Single-Pass Arc Welds", *Welding Journal*, Vol. 79. No. 5, May 2000 121_s – 125_s.

[8] P. W. Fuerschbach. *Welding Journal*. Vol. 75: January, 1996; 24_s – 34_s

[9] M. R. Frewin, D. A. Scott, *Welding Journal*, January 1999, 15_s – 22_s.

[10] P. Tekriwal and J. Mazumder, *Welding Journal*, July 1988, 150_s-156_s.

Biographic Information

Dr. Edison BONIFAZ CONTO. Dr. Bonifaz Conto is Professor of Materials Engineering, Physical Metallurgy of Welding and Numerical Analysis in the Mechanical Engineering Department at University San Francisco de Quito-Ecuador.

Dr. Ernesto INDACOCHEA. Dr. Indacochea is Professor in the Dept. of Civil and Materials Engineering at the University of Illinois at Chicago.

Authorization and Disclaimer

Authors authorize LACCEI to publish the papers in the conference proceedings on CD and on the web.